Evidence of the 17-keV neutrino in the β spectrum of ^{35}S

J. J. Simpson and A. Hime*
Department of Physics and Guelph-Waterloo Program for Graduate Work in Physics, University of Guelph, Guelph, Ontario, Canada N1G 2W1
(Received 9 September 1988)

Two measurements of the β spectrum of ^{35}S have been made using a windowless Si(Li) detector. The data show a clear threshold anomaly at $Q-17$ keV which is consistent with the emission of a 16.9±0.4 keV neutrino with a mixing probability of (0.73±0.09±0.06)%. All values of mixing probability $<0.26\%$ are rejected at the 99% confidence level.

I. INTRODUCTION

In 1985 a distortion in the low-energy region of the β spectrum of tritium implanted into a Si(Li) x-ray detector was reported[1,2] and interpreted as due to the emission of a heavy neutrino of mass about 17 keV. The mixing probability of this heavy neutrino was estimated to be between 2% and 4%. A number of authors pointed out[3–5] that the effective screening potential used (99.4 eV) in correcting the Fermi function, according to Rose's method,[6] was too large and that a potential of about 65.4 eV is correct for free tritium in a total-absorption measurement. A reduction in the screening potential has the effect of reducing the mixing probability.

If the distortion seen in tritium is due to the emission of a heavy neutrino, a similar distortion should be seen in other β spectra. Very soon after the first paper on tritium appeared, a number of reports[7–11] describing experiments with ^{35}S were published, all of which claimed no evidence for a distortion due to a 17-keV neutrino with mixing probabilities, in some cases, down to 0.15%. However, many of these experiments have been criticized and several have been reinterpreted[2,12] to suggest that they are in fact consistent with the emission of a 17-keV neutrino. Very recently, an experiment on ^{63}Ni has been reported[13] claiming an upper limit of 0.3% for a 17-keV neutrino branch, consistent with the claims of the ^{35}S experiments.

In order to settle the obvious disagreements, two experiments have been carried out. In the first, a hyperpure Ge x-ray detector was implanted with tritium, in a manner similar to that described in Ref. 1. This experiment, which resolves a number of questions unresolved by the earlier one, shows a distortion consistent with the Si(Li) detector results, and is described in an accompanying publication.[14] This paper includes discussion of screening effects in ^{3}H alluded to above. The second experiment, a measurement of the β spectrum of ^{35}S, is reported here.

II. THEORETICAL CONSIDERATIONS

The idea of the mixing between neutrino-antineutrino mass eigenstates, first introduced by Pontecorvo,[15] was extended by Katayama, Matsumoto, Tanaka, and Yamoda[16] and Maki, Nakagawa, and Sakata[17] to mixing of two flavors of neutrinos. Nakagawa, Okonagi, Sakata, and Toyoda[18] pointed out that such mixing can cause changes in the Kurie plots of allowed β decays provided the β-decay Q value is large enough. Recently, Shrock,[19] McKellar,[20] and Kobzarev, Martemyanov, Okun, and Schepkin[21] have discussed the effect on β spectra of the mixing of three or more flavors of massive neutrinos. The present discussion will be limited to the mixing of only two flavors.

Consider the case where the electron neutrino is a linear combination of two mass eigenstates $|\nu_1\rangle$ and $|\nu_2\rangle$ of masses M_1 and M_2:

$$|\nu_e\rangle=\cos\theta|\nu_1\rangle+\sin\theta|\nu_2\rangle\ .$$

The orthogonal combination of $|\nu_1\rangle$ and $|\nu_2\rangle$ is assumed to be $|\nu_\mu\rangle$, $|\nu_\tau\rangle$, or perhaps a fourth-generation neutrino. The β spectrum is then

$$\frac{dN(E)}{dE}=\frac{dN(E,M_1)}{dE}\cos^2\theta+\frac{dN(E,M_2)}{dE}\sin^2\theta\ , \quad (1)$$

where $dN(E,M)/dE$ is the usual β-energy spectrum for allowed decay with the emission of one neutrino of mass M:[22]

$$\frac{dN(E,M)}{dE}\propto pE[(W-E)^2-M^2]^{1/2}(W-E)F(E,Z)\ . \quad (2)$$

Here, W is the total energy available for the transition and E and p are the total energy and momentum of the β particle. The mass M (in energy units) must be less than $(m_x-m_y-m_e)$ where m_x, m_y, and m_e are the masses of the parent nucleus, daughter nucleus, and the electron (neglecting differences in atomic binding energies). The Fermi function $F(E,Z)$ accounts for the Coulomb interaction between the emitted β particle and the charge Z of the daughter nucleus.

The Kurie plot for an allowed spectrum

$$K\equiv\left[\frac{dN(E,M)/dE}{pEF(E,Z)}\right]^{1/2} \quad (3)$$

is linear when $M=0$ and extrapolates to an energy W, or in terms of kinetic energies to an energy $Q=W-m_e$. For nonzero M, the Kurie plot is linear in energy regions sufficiently below the energy $Q-M$ and still extrapolates to an energy Q, but as the energy nears $Q-M$ from below the slope increases until it is vertical at the end

point of the β spectrum. If the true β spectrum is given by $dN(E)/dE$ of Eq. (1), then the Kurie plot will be a superposition of two Kurie plots as shown in Fig. 1. The Kurie plot is said[19] to have a "kink" where it abruptly ends for nonzero neutrino mass and the size of the kink determines $\sin^2\theta$. The mass M_1 has been taken to be zero.

The energy region over which the Kurie plot is substantially nonlinear (the kink region) is not very large in units of M_2 as can be judged from the expression[1]

$$\frac{\Delta K}{K} \sim \frac{\sin^2\theta}{2}\left[1-\frac{M_2^2}{(Q-E)^2}\right]^{1/2} \tag{4}$$

or from Fig. 1. Here ΔK is the deviation of the Kurie plot from a straight line. In such a narrow energy region, it is often difficult to get enough statistical accuracy to measure a kink reliably, especially if $\sin^2\theta$ is small. It is possible to obtain evidence for M_2 by measuring the β spectrum over regions above and below $Q-M_2$ and noting that the slope of the Kurie plot is different in the energy region above $Q-M_2$,

$$\frac{dK}{dE} \propto \cos\theta, \quad E > Q-M_2 , \tag{5}$$

from well below (by about an energy M_2)

$$\frac{dK}{dE} \propto 1, \quad E \lesssim Q-2M_2 . \tag{6}$$

This feature has primarily been the basis of all the ^{35}S and ^{63}Ni measurements to date, and will be discussed further below.

III. EXPERIMENTAL DETAILS

A. Spectrometer

A commercial Si(Li) detector of 200 mm^2 active area (containing some ^{3}H from a previous implantation) was removed from its cryostat and mounted in a vacuum chamber as shown in Fig. 2. This detector operates at liquid-nitrogen temperature with a cold field-effect-transistor (FET) package to optimize resolution. Open sources of ^{35}S were prepared by depositing solutions of high specific activity on Mylar substrates that are 10 μm thick. These substrates are covered by a thin aluminum or gold coating so that the source can be grounded during the course of a measurement. Calibration sources of ^{57}Co were prepared in a fashion similar to the ^{35}S sources.

The vacuum was maintained at pressures of $\sim 5\times 10^{-5}$ mbar using liquid-nitrogen-cooled molecular sieves. In addition, a copper cryopanel of $\sim$300 cm^2 surface area surrounds the silicon detector and is cooled to liquid-nitrogen temperature through a copper cold finger. This provides a large cold surface that freezes out residual water vapor in the chamber that can otherwise freeze on the detector surface. Without this cold surface a continuous ice build-up on the detector took place as observed by a continuous energy shift of the internal conversion electron lines of ^{57}Co. The centroid positions and shape of these lines remain sufficiently stable for periods of 4–5 days with the copper cryopanel in place.

The main source of distortion of a β spectrum in the present type of spectrometer is primarily the saturated backscatter or back-diffusion of the incident electrons by inelastic scattering from electrons in the Si(Li) crystal. Many experiments have been carried out to measure the fraction of electrons backscattered from thick absorbers and are summarized by Knop and Paul.[23] Measurements show that about 15% of a parallel beam of incident electrons are backscattered from silicon and about 30% for a diffuse source of electrons, which is close to the present experimental situations. The backscatter fraction is also found to be essentially independent of energy. The energy left in Si(Li) detectors by the backscattering electrons has also been measured. In particular Planskoy[24] has measured the backscatter fraction and the shape of the energy distribution in a Si(Li) detector with an experimental arrangement very similar to the present one. He finds for diffuse scattering of 164-keV electrons a backscatter fraction of 32%. This fraction includes any low-

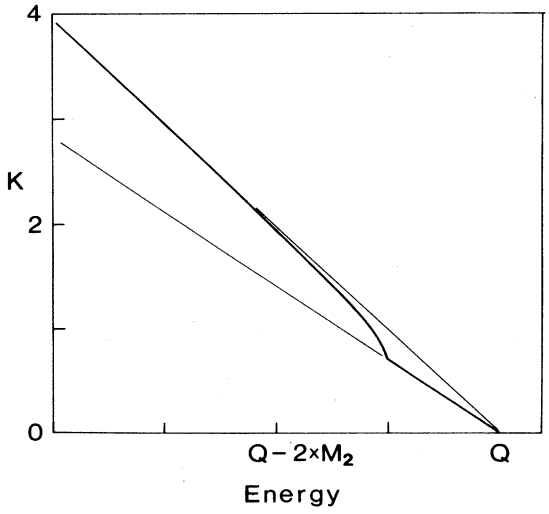

FIG. 1. Schematic of a Kurie plot with the emission of a two-component neutrino, with $M_1=0$ and $\sin^2\theta=0.5$.

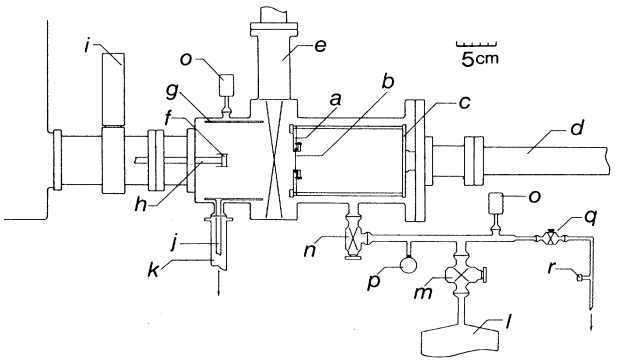

FIG. 2. Schematic of the spectrometer. *a*, acrylic source holder; *b*, source; *c*, source-holder mount; *d*, source manipulator; *e,m,n,q,r*, vacuum valves; *f*, Si(Li) crystal; *g*, cryopanel; *h,j*, cold fingers; *i*, preamplifier; *k,l*, sorption pumps; *o,p*, vacuum gauges.

energy electrons which backscattered inelastically from his Vyns source backing (thickness not specified) and from the vacuum chamber walls, but nevertheless the result is in good agreement with Ref. 23 above. The energy distribution[24] of inelastically backscattered electrons of a 624-keV diffuse source is essentially flat above 10% of full energy, and for a parallel beam of 300-keV electrons is flat above about 70% of full energy. Recently von Dincklage and Gerl[25] have shown that the inelastically scattered electrons of a diffuse source of 973-keV electrons is essentially flat at least above 30% of full energy.

B. Sources

Source substrates were prepared by stretching ~ 10-μm Mylar foils across a 25.4-mm-diameter aluminum ring. A second, concentric ring was then used to hold the substrate in place. The source substrate is mounted on an acrylic disk and fastened at the back with a separate piece of acrylic in the shape of an annulus. This acrylic disk is, in turn, mounted in line with the detector by a thin aluminum ring held by four, 125-mm-long aluminum rods. In this way there is no material in the immediate vicinity behind the source, apart from the 10-μm Mylar substrate, from which β particles can scatter when emitted in the backward direction. When recording spectra, the sources are moved close to the Si(Li) detector so that the acrylic disk acts to shield the detector from backscattering from the cryopanel and much of the vacuum vessel.

The Mylar backings are thicker than desirable for β spectroscopy using magnetic spectrometry, having a thickness of about $\frac{1}{20}$ the extrapolated range of 160-keV electrons, but this thickness is less than 13% of that required to reach saturation backscattering, according to Ref. 23. At saturation, the backscattering fraction from Mylar is about 10%, so that the present Mylar backings could contribute a 2–3 % continuum distribution below the full energy peak for a monoenergetic electron. Bothe[26] has shown that this distribution, from low-Z elements such as carbon, is essentially symmetric about an energy one-half the full energy. Hence the contribution of the Mylar to the backscattered tail of the electron distribution is small compared to that from the detector itself and will be included as part of the electron response function in the analysis.

Elastic scattering from atoms could produce a tail from the full energy down to the full energy minus twice the energy loss in the Mylar, about 10 keV. However, the cross section for elastic scattering is very small[27] and it would contribute less than 0.04% of the direct electrons.

The sources were prepared by chemical adsorption of insoluble compounds of radionuclides as described by Wyllie and Lowenthal.[28] A ~ 0.5-μCi source was prepared on aluminized Mylar by precipitation with barium nitrate from a sodium-sulfate solution in water (specific activity 447 mCi/mmol and $<8\times10^{-4}$% radioactive contaminants). A stronger source (~ 5 μCi) was prepared on Au-coated Mylar from a carrier-free solution of sulfuric acid in water (containing $<1.5\times10^{-4}$% radioactive contaminants). In both cases the diameter of the source area was about 10 mm. Source properties are given in Table I. The thickest source has an estimated average energy loss to 150-keV electrons of 0.6 eV.

Calibration sources of ^{57}Co were prepared in a similar way on Au-coated Mylar from a carrier-free solution of cobaltous chloride in 0.1M HCl by precipitation with potassium hydroxide. One source had an activity of ~ 1 μCi and an estimated thickness of $\sim 10^{-10}$ g/cm^2, about the same thickness as the stronger sulfur source. A second source of ^{57}Co was also prepared with an order of magnitude more activity. There were no observable differences in the position or shape of the internal-conversion (IC) electron lines between the two ^{57}Co sources indicating that source thickness effects are negligible for these two sources, and by inference for the stronger ^{35}S source.

Care was taken in the preparation of all sources to make sure that no material was deposited on the back of the Mylar. In addition, the spectra of the ^{57}Co sources were examined for evidence of source material on the back and an upper limit of <0.2% can be placed on the fraction of electrons that could be coming through from the back. Finally, the two very different sources of ^{35}S were used in different runs and as we shall see, the results of these two runs are very similar, suggesting that a negligible fraction at most might be on the back.

C. Spectrum recording

Pulses from the detector preamplifier were amplified and shaped by an Ortec 572 amplifier operating with 3-μs shaping time constants. In order to reduce the number recorded of chance occurrences of two, nearly simultaneous β particles entering the detector (pile-up), the analog-to-digital converter (ADC) analyzing the amplifier pulses was gated off by a signal from a pile-up inspector (Ortec 404A) operating with an inspection interval of 16 μs.

A preliminary run (run A) was made using the weak ^{35}S source to monitor the stability of the spectrometer and systematics associated with the measurement. A ^{35}S spectrum was recorded continuously for a three-day period, at the beginning and end of which ^{57}Co calibration data were acquired. The ^{57}Co source was placed in the same position that the ^{35}S source occupied. There were no observable differences in the position and/or shape of the IC electron lines between ^{57}Co spectra accumulated at the beginning and end of this three-day period, indicating that the sources prepared are stable and that there was no significant ice build-up on the detector surface. In addition, there was no change in the

TABLE I. Properties of ^{35}S sources used.

Substrate	Activity (μCi)	Estimated source thickness (g/cm^2)	Run	Source-detector distance (mm)	Count rate (cps)
Al-Mylar	0.5	3.7×10^{-7}	B	9	2100
Au-Mylar	5.0	7.8×10^{-10}	C	35	2100

ambient background signal or source count rate which suggests that the source activity remains bound to the substrate at the vacuum pressure maintained.

The stability of the spectrometer could be maintained for a fourth day; however, by the fifth day slight tailing effects were observed in the internal conversion lines arising from the slow build-up of ice on the surface of the detector. At this point the detector was allowed to warm up to room temperature to rid it of the ice layer. After the detector was cooled to liquid-nitrogen temperature the response of the detector to the ^{57}Co electrons had returned to its original form. As a result, the longer runs described and analyzed below were restricted to three-day cycles, at the end of which the detector was warmed to room temperature. Calibration measurements were made at the beginning and end of each cycle. Two long runs were made (runs B and C) of $\sim 1.2\times 10^6$ s each with a count rate in each run of 2100/s. In run B the weaker ^{35}S source deposited on aluminized Mylar was used and positioned ~ 9 mm from the detector. Data were accumulated in a TN-7200 multichannel analyzer up to an energy of 230 keV with a dispersion of ~ 225 eV/channel. Run C was made with the stronger ^{35}S source deposited on gold-plated Mylar and placed ~ 35 mm from the detector. In this case pulses were analyzed by a TN-4000 multichannel analyzer incorporating a TN-1242 ADC, up to an energy of 470 keV with a dispersion of ~ 231 eV/channel.

Calibration of the spectrometer was established using the γ rays of ^{57}Co supplemented with pulses from a precision pulser (BNC model PB-4). The calibration was taken to be linear since the addition of a quadratic term did not change the determined energies by more than ~ 2 eV over 230 keV. The K IC electrons of the 122- and 136-keV γ rays were used to monitor the resolution of the detector for fully absorbed electrons (see Fig. 3). The resolutions were 1.40 keV and 1.51 keV [full width at half maximum (FWHM)], respectively, while those of the corresponding γ rays were 0.77 keV. The IC lines are shifted 2.44 keV lower than their expected positions due partially to a dead layer on the front of the detector ≈ 1.4 μm (Ref. 29) and partially due to the -1.5-kV bias voltage on the front of the detector. The wider resolution of the IC line compared to the γ-ray line implies a Landau straggling width of about 0.95 keV (Ref. 23).

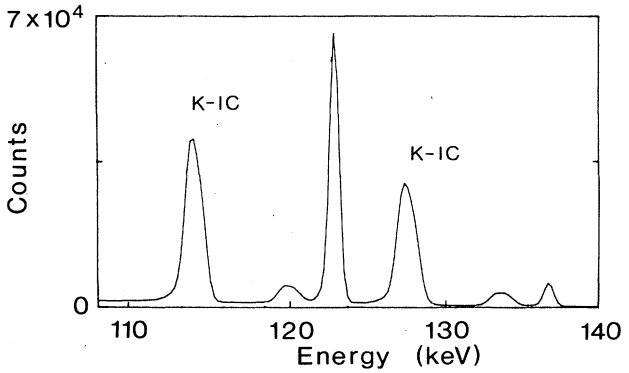

FIG. 3. ^{57}Co calibration spectrum. The peaks marked K-IC are the K conversion lines of the 122- and 136.4-keV γ rays.

IV. EXPERIMENTAL RESULTS

A. Background

Figure 4 shows a logarithmic display of the β spectrum of run C above about 90 keV, including about 150 keV of background. There are two main sources of background, unrejected pile-up pulses, and ambient background consisting primarily of Compton-scattered γ rays. The ambient background was measured with source removed and is adequately described by a linear function. Using a random pulser (BNC model DB-2) it was determined that at an average rate of 2500 cps unrejected pile-up consists primarily of two pulses occurring so close in time that the piled-up pulse is encoded at a pulse height equal to the sum of the two individual pulse heights. Only one in a thousand pile-ups occurs with a pulse height lower than this. Furthermore, the fraction of unrejected pile-up pulses is constant as a function of pulse height. Using these facts a spectrum of unrejected pile-up pulses was calculated by summing each pulse with all others. This used the entire spectrum from zero energy by quadratically extrapolating from the noise level (~ 0.8 keV) down. The combination of pile-up plus linear background was fitted to the region above the end of the β spectrum by varying the slope and intercept of the linear function and the overall normalization of the pile-up spectrum. The result is shown as the smooth curves in Fig. 4, and the residuals of the fit are shown in Fig. 5. A second iteration of the pile-up spectrum was also made, but the shape of the resulting pile-up spectrum was essentially identical to the initial one. This is because the amount of unrejected pile-up is extremely small, $<0.3\%$ of the β spectrum.

The fitted background was subtracted from the β spectrum at this point because the β pulses must be shifted up in energy to account for the shift observed in the IC lines. Because the electron stopping power is not constant over the energy region of interest,[29] the data have been shifted

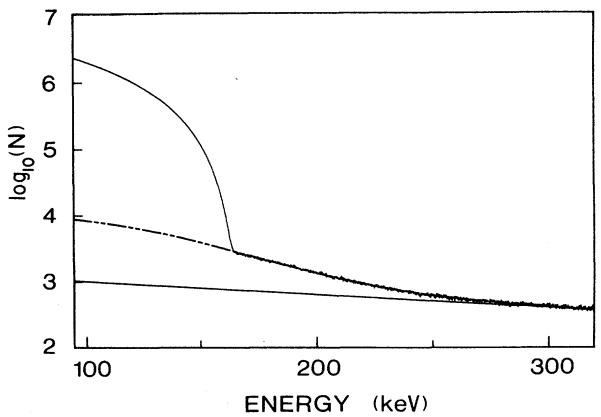

FIG. 4. A portion of the data of run C, showing the background extending up to 330 keV with the fit to the background based on a model of ambient background (smooth curve) plus pile-up (dashed-curve); see text.

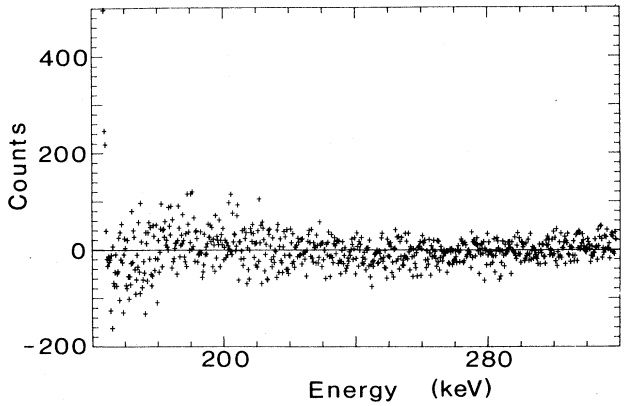

FIG. 5. Background residuals for run C, defined as experimental minus fitted number of counts. $\chi^2/\nu=1.12$ with $\nu=646$.

by amounts varying from 2.5 keV at the low-energy end to 2.3 keV at the high-energy end of the analyzed region, 110–166 keV, and the number of counts at each energy have been corrected for the changing dispersion. Finally, to smooth out systematic periodicities that were observed in the ADC channel widths, the data were binned by groups of three, yielding a dispersion of $\sim$700 eV/channel. In each of runs B and C there are about 4.5×10^5 β particles per 700 eV at 150 keV. At this energy the background plus pile-up is 1.3×10^4 counts.

B. Data analysis

The theoretical β spectrum was represented by Eq. (1) above using a modified nonrelativistic Fermi function of the form

$$F(E,Z)=X(1-e^{-x})^{-1}f((v/c)^2)\ , \tag{7}$$

where

$$X=\frac{2\pi Z\alpha}{v/c}$$

and

$$f((v/c)^2)=1.117\,56-0.049\,68(v/c)^2+0.020\,40(v/c)^4\ .$$

Here Z is the charge of the daughter nucleus, v/c is the β-particle speed relative to that of light, and α is the fine-structure constant. The function $f((v/c)^2)$ makes the values of this Fermi function agree to within one part in 10^5 with the tabulated values of the relativistic calculation of Behrens and Jänecke[30] over the energy range of interest for the present experiment. A screening correction has been made using Rose's method[6] with a screening potential of 1.73 keV. The data were analyzed by fitting them to this theoretical β spectrum convolved with the response function for electrons. Based on the discussion of Sec. III A above, the response function was taken to be a Gaussian function with a flat tail extending to zero energy, the relative area of this tail being kept the same for all incident energies. This is a reasonable approximation to previous experiments in view of the narrow energy range, 110–166 keV, to be fitted.

A measurement of the number of incident electrons backscattered from the Si(Li) detector has been made using the ^{57}Co source (Fig. 3). The ratio of the counts detected in the full energy peak of electrons from K internal conversion of the 122-keV γ ray to the number in the 122-keV γ-ray peak, $n_K(122)/n_\gamma(122)$, depends on the fraction of electrons not backscattered $(1-f_{\rm bs})$ and therefore which leave their full energy in the detector, as well as on a number of other factors including efficiencies, internal-conversion coefficients, branching fractions, and solid-angle factors. At a distance of 35 mm, this ratio is relatively simple,

$$\frac{n_K(122)}{n_\gamma(122)}=\frac{\alpha_K}{\epsilon_\gamma}(1-f_{\rm bs})\ ,$$

since the solid angle of the detector is essentially the same for both electrons and γ rays and the correction factor for coincidence summing of γ rays, x rays, and IC electrons is only 0.4%. The factor α_K is the K IC coefficient,[31] 0.0218±0.0012 and ϵ_γ is the photopeak efficiency for a 122-keV γ ray in the Si(Li) detector which has been determined to be 0.0148±0.0007. The measured ratio is 1.044±0.007, thus yielding the fraction of 115-keV electrons backscattered from the Si(Li) detector $f_{\rm bs}=0.29\pm0.05$, in good agreement with the results of Planskoy[24] and earlier measurements.[23] In addition, this result is free of backscattering from the source backing or vacuum chamber.

The full-energy part of the response function for incident electrons was estimated from the observed widths of the IC lines of calibration sources. Although straggling in the dead layer of the detector produces a nonsymmetric energy distribution[32] the IC lines are sufficiently symmetric that they have been represented by a Gaussian function. The Gaussian part of the response function for the highest-energy β particles has been estimated to have a σ between 0.67 and 0.76 keV. This estimate is made by determining the statistical width from the ^{57}Co γ rays and then convoluting this with a Landau distribution obtained from the ^{57}Co IC lines. Two estimates of the Landau width at 166 keV, one the same as that from the ^{57}Co lines and the other scaled inversely as the square of the β velocity, give the range of the estimation. It also includes resolution broadening due to long-term drifts which was included by summing all the calibration runs, and due to binning the data. There was no observable difference in the ^{57}Co peak shapes as a function of counting rate from 300 to 1300 counts per second.

In the analysis, both σ of the Gaussian and the area of the flat tail are allowed to vary.

C. Results

Runs B and C have been analyzed separately to look for systematic effects. However, for display purposes they have been combined, taking into account their slightly different energy calibrations, and Fig. 6(a) shows the shape function obtained by taking the ratio of the experimental β spectrum to the best-fitting theoretical spectrum with $R\equiv\sin^2\theta=0$ convolved with the response function described above. It is readily apparent that the shape function is not constant, as it should be for allowed

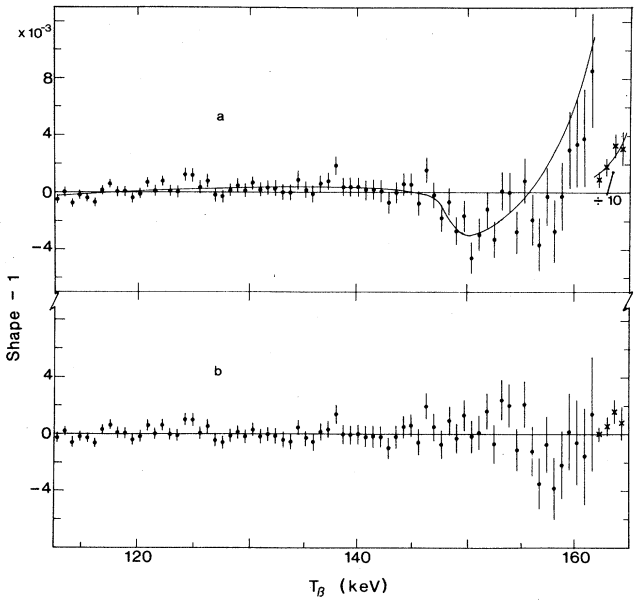

FIG. 6. The deviation of the shape function from a constant for the combined data of runs B and C. In (a) the theoretical spectrum has $\sin^2\theta=0$. $\chi^2/\nu=2.0$. The smooth curve shows the shape expected for $M_2=17$ keV and $\sin^2\theta=0.008$. In (b) the experimental data are divided by a theoretical fit with $M_2=17$ keV and $\sin^2\theta=0.0075$. $\chi^2/\nu=1.0$.

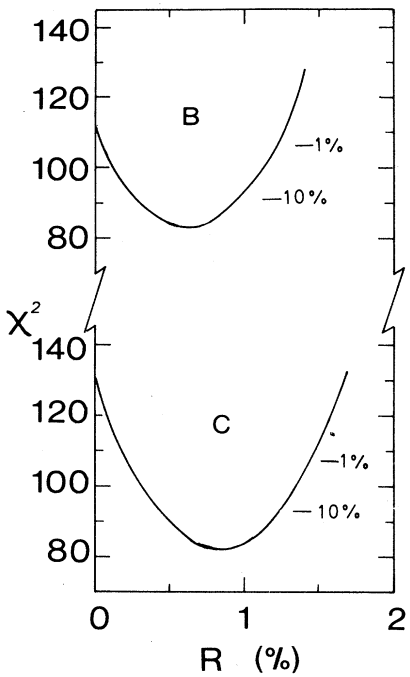

FIG. 7. χ^2 curves for fits to the two ^{35}S experiments B (number of degrees of freedom $\nu=75$) and C ($\nu=77$) vs 17-keV neutrino mixing probability $R\equiv\sin^2\theta$ over the energy region 110–166 keV. For each value of R used to attempt a fit, the normalization, end-point energy, and the tail of the response function were varied.

decay, but that it looks very much as the smooth curve which is the shape function expected if there is a 17-keV neutrino emitted with $\sin^2\theta=0.8\%$. Figure 6(b) shows the shape function when the experimental β spectrum is divided by the fitted theoretical spectrum including a 17-keV neutrino with $\sin^2\theta=0.75\%$.

The distribution of χ^2 as a function of $\sin^2\theta$ is shown in Fig. 7 for both runs B and C and it is seen that there is a deep minimum, for $M_2=17$ keV, near $\sin^2\theta=0.007$, and $\sin^2\theta=0$ is completely ruled out. Table II lists the results of the fits to runs B and C.

In these χ^2 curves, all parameters have been varied except M_2 and σ. The values of σ used are found to give the minimum in χ^2 and are in reasonable agreement with expectation. At $\sin^2\theta=0$, the variation of χ^2 with σ has been studied and, for example, for run C, χ^2 has a minimum at a value of 106 at σ of 0.9 keV. As well as not giving the lowest value of χ^2, this σ would seem to be physically too large, as it is as large as that observed for the K-conversion electrons of ^{137}Cs at 624 keV (see also Sec. IV below). In spite of similarity in source fabrication techniques, there might still be concern that the electron resolution for the β particles is different from that of the ^{57}Co IC electrons. However in this work two ^{35}S sources, of very different thicknesses, have been used and the results are essentially identical with the exception that the best estimate of σ increases from 0.76 to 0.8 keV for the thicker source. This increase is due primarily to geometry differences since the detector dead layer appears slightly thicker in the closer geometry. Shake-up of atomic electrons in the daughter chlorine atom and shake-off of L electrons[33] will broaden the resolution relative to the IC lines of ^{57}Co, but by $<1\%$.

A linearly varying σ, fitting the measured value at 115 keV and with $\sigma=0.76$ keV at 166 keV, has also been tested and gives essentially identical results to the constant σ analysis, except for a very slight shift in Q.

TABLE II. Results of fits to the two ^{35}S β spectra.

Run	Mixing probability $\sin^2\theta$	End-point energy Q (keV)	Gaussian width σ (keV)	Backscatter fraction f_{bs}	Quality of fit χ^2/ν	Confidence level (%)
B	0	166.53	0.80	0.319	1.46	0.43
	0.0063±0.0013	166.57	0.80	0.317	1.09	25.2
C	0	166.71	0.76	0.296	1.66	0.012
	0.0084±0.0013	166.74	0.76	0.291	1.03	40.0

A major difference in runs B and C is the source-detector distance. The same ^{57}Co source that was used to estimate the backscatter fraction for run C described in Sec. IV B was also placed in the same position as the ^{35}S source of run B. An analysis similar to the above, but slightly more complicated due to increased coincidence summing, to increased importance of the finite area of the source, and to differences in the effective solid angle of the detector for electrons compared to γ rays (because the electrons only penetrate the first 100 μm of the crystal whereas the photons easily illuminate the entire thickness), was carried out. Assuming the true far-distance backscattered fraction is 29.1% as measured in run C and which is in very good agreement with the value determined by the ^{57}Co source in Sec. IV B, the analysis yields (35.2±1.9)% as the near-distance backscattered fraction in reasonable agreement with the 31.7% from fitting the ^{35}S data of run B. Any difference might indicate that, in the ^{35}S experiment, a few percent of the fitted 29.1% in the far-source position is backscattering from the walls of the chamber, whereas in the close source position this fraction will become a negligible proportion because the source-detector solid angle is a factor of 10 larger. In conclusion, the backscattered fraction that is obtained by fitting the ^{35}S spectra is in very good agreement with the measurements using a ^{57}Co source both in absolute intensity and in distance variation, and is in good agreement with previous measurements quoted in Sec. III A. This agreement confirms the estimate that backscattering from the source backing will have a very small effect, and confirms that the assumption of a flat tail is also reasonable. If, for example, the tail had a significant slope then the ^{57}Co backscattered fraction and the ^{35}S backscattered fraction would be in disagreement because in ^{35}S the entire tail is estimated by fitting over only a limited energy region from 110 to 166 keV. [See also item (2) in Sec. IV D.]

Combining the fits of runs B and C gives an estimated M_2 of 16.9±0.4 keV and $\sin^2\theta=(0.73\pm0.09)\%$. Furthermore, all values of $\sin^2\theta<0.26\%$ are rejected at the 99% confidence level. The hypothesis that there is only a one-component neutrino is rejected at the $(100-5.1\times10^{-4})\%$ level using the best-fitted σ parameter. If one ignores the *a priori* evidence on σ and allows it to increase to find the minimum in χ^2 at $\sin^2\theta=0$, then the one-component neutrino hypothesis is still rejected at the 99.4% level.

Narrow regions 135–165 keV and 140–160 keV have also been analyzed. The broader of these two regions gives results that are nearly identical to the full-range analysis described above. Figure 8 presents the combined χ^2 curves for runs B and C for the narrower energy region, holding the electron response functions fixed at the values determined above. Minimum χ^2 occurs at $\sin^2\theta=0.6\%$ and $\sin^2\theta=0$ is ruled out at the 98.4% level. Thus, the distortion in the β spectrum at 150 keV does not arise from an arbitrary choice of fitting region.

D. Variations in parameters

In fitting β spectra, there are many parameters apart from the neutrino parameters that must be varied and this section gives a brief survey of how the various parameters influence the fitting.

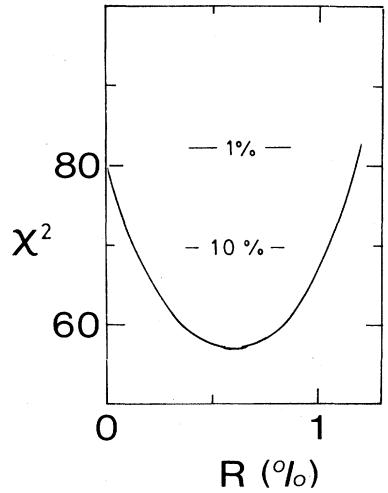

FIG. 8. Combined χ^2 curve for fits to runs B and C ($\nu=56$) vs 17-keV neutrino mixing probability R over the energy region 140–160 keV.

(1) End-point energy. The quality of the fit is very sensitive to the end-point energy Q. Figure 9 shows χ^2 curves for two cases, $\sin^2\theta=0$ and $\sin^2\theta=0.008$. It is very clear that Q must be varied significantly to find the best fit for different values of $\sin^2\theta$, and that *a priori* knowledge of Q at a sufficiently accurate level ($\sim$ a few eV) is almost certainly impossible.

(2) Backscatter fraction. χ^2 curves for the backscatter fraction f_{bs} for two cases, $\sin^2\theta=0$ and $\sin^2\theta=0.008$ are shown in Fig. 10. Q has been varied to obtain the minimum χ^2 in each case. The minimum is very sharp

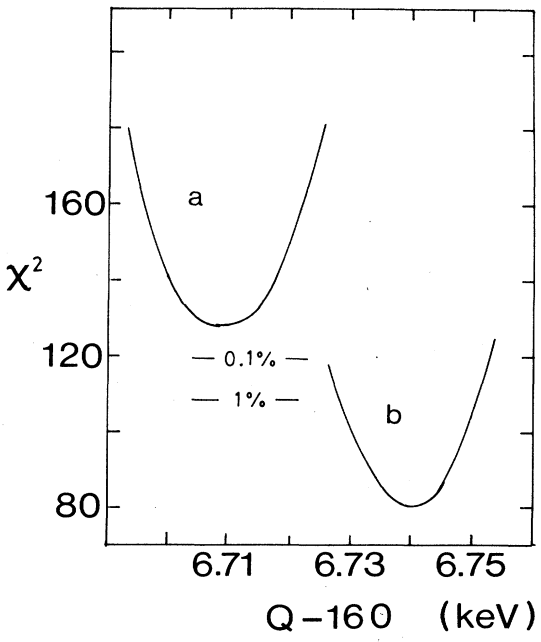

FIG. 9. χ^2 for the fit to run C vs end-point energy Q. Curve a is for $\sin^2\theta=0$ and curve b is for $\sin^2\theta=0.008$.

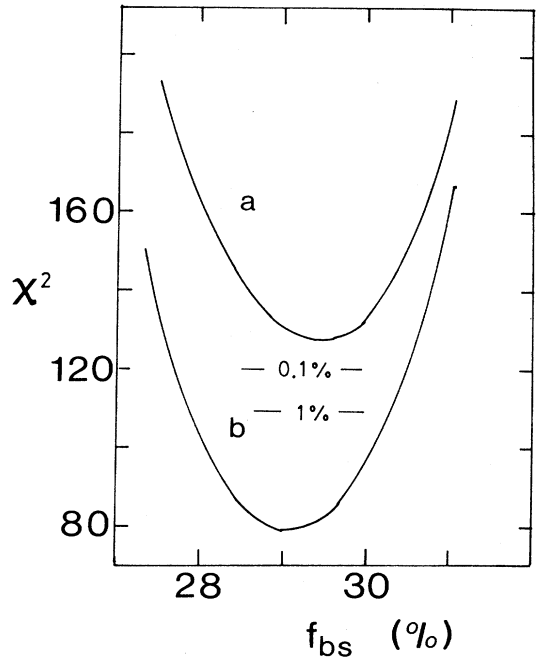

FIG. 10. χ^2 for the fit to run C vs backscatter fraction f_{bs}. Curve *a* is for $\sin^2\theta=0$ and curve *b* is for $\sin^2\theta=0.008$.

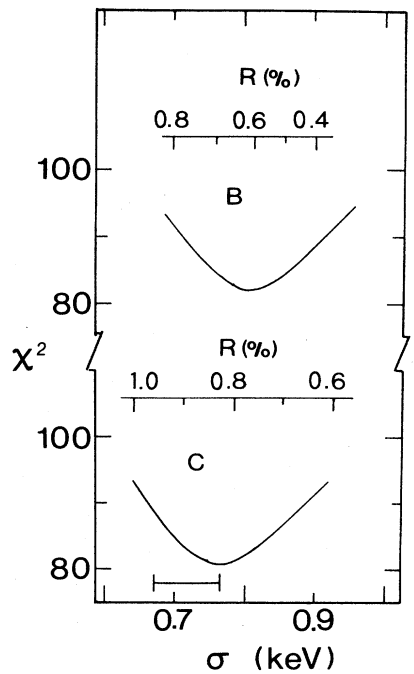

FIG. 11. χ^2 for the fit to runs B and C vs σ of the Gaussian part of the electron-response function. The upper abscissa gives the value of R which minimizes χ^2 at each value of σ. The bar at the bottom of the figure shows the expected value of σ based on the ^{57}Co lines (see Sec. IV B).

but it is essentially at the same value of f_{bs} for all relevant values of $\sin^2\theta$. However, it would be extremely difficult, if not impossible, to measure f_{bs} in a separate experiment to the accuracy required.

In addition, a flat backscatter tail with an inverted parabola on it, the latter amounting to 10% of the backscatter fraction and peaking at one-half the incident electron energy, has also been tried. This would simulate a large amount of backscattering from the source backing. It was found that this change caused χ^2 to increase to about 155 at $\sin^2\theta=0$.

(3) Gaussian resolution. A χ^2 curve of resolution parameter σ is presented in Fig. 11. The end-point energy and $\sin^2\theta$ are varied, and along the top abscissa the value of $\sin^2\theta$ at the minimum is shown. The minimum is not very sharp and there is some correlation with $\sin^2\theta$. However, σ at the minimum is close to the estimated value of σ. If for run B σ were constrained to the *a priori* upper limit of 0.76 keV, $\sin^2\theta$ would increase to about 0.73%.

(4) Background. The background fitted above the end of the β spectrum has three parameters, the two coefficients of the linear ambient background and the normalization of the unrejected pile-up spectrum. The sensitivity to this background has been tested in two ways. In one, the background was shifted up and down by a constant number of counts equivalent to about one standard deviation in each of the parameters working in the same direction. On the scale of the residuals shown in Fig. 5, this is equivalent to a shift of a constant 35 counts, which is an enormous increase in χ^2/ν for the fit to the background. In a second test, the linear background was held fixed and the normalization of the pile-up spectrum was changed by one standard deviation. The only significant change was induced by the constant increase in the background, which reduced $\sin^2\theta$ from 0.84% to 0.72% for run C. The results are thus rather insensitive to large and unlikely errors in the background.

(5) Energy shift. The energy-dependent shift applied to the β spectrum has been changed from the range 2.5–2.3 keV used above to 2.6–2.2 keV, to test the sensitivity of the results to the shift. The only effect on the results is to decrease the end-point parameter from 166.74 keV down to 166.45 keV and to increase f_{bs}, for example, from 29.1% to 30.7% in run C. The value of $\sin^2\theta$ remains essentially unchanged.

E. *K*-shell shakeoff

As mentioned above, shake-up and *L*-shell shakeoff will contribute a slight broadening to the Gaussian part of the electron response function which is small and is included in the fitting. However, shakeoff of the *K* electron from the daughter Cl atom will also occur. It is known[34] that the atomic matrix element which controls the shakeoff is strongly peaked at the binding energy of the *K* shell, so that as a good approximation the spectrum of β particles accompanying the shakeoff electron will look as the original β spectrum shifted down by 2.8 keV. Most of the shaken-off electrons are too low in energy to be registered in the detector. For ^{35}S, the total intensity of *K*-shell shakeoff is measured to be $\sim$0.22% of the total decay rate.[34] The effect of shakeoff has been simulated by subtracting from the measured β spectrum a 0.22% fraction of itself shifted down by 2.8 keV. There was at most

a downward shift in $\sin^2\theta$ of 2×10^{-4} and the minimum χ^2 was about as good.

V. DISCUSSION

A. Present results

A threshold anomaly 17 keV from the end point in the measured ^{35}S spectra from that expected from theory for the emission of a single-component massless neutrino is the only distortion observed in the spectrum over the energy interval ranging from 110 to 166 keV. The agreement between experiment and theory below this anomaly indicates that the systematic effects associated with the technique of the measurement, including detector response function and background, are well understood. It is very unlikely that systematic uncertainties would affect the shape of the spectrum in only an isolated region and not continuously over the entire β spectrum. It must be emphasized that *no arbitrary* shape factor has been required in analyzing the ^{35}S spectra to achieve a good fit, reinforcing confidence in the knowledge of the systematic features governing the shape of the measured spectrum. In this regard, it should be noted that the same backscatter fraction is obtained if we confine the fitting region to energies below about 145 keV where the effect of neutrino mass is insignificant. This can be confirmed by comparing Figs. 6(a) and 6(b). The β decay of ^{35}S is an allowed transition and variation in the shape arising from higher-order terms in the nuclear matrix element are at the level of 0.01% (Ref. 35).

The distortion observed in the β spectrum of ^{35}S is best represented by a two-component model with the emission of a 16.9 ± 0.4 keV neutrino with a $(0.73\pm0.09\pm0.06)\%$ mixing probability, where the second error includes systematic uncertainties in σ, in the background and shakeoff. This result is in reasonable agreement with the distortion observed in several tritium spectra,[1,2,14] although the best estimate of the mixing probability for a heavy neutrino is slightly higher in the case of ^{3}H. However, in the case of ^{3}H the phase space available for the emission of a 17-keV neutrino is very small and, combined with its low energy of β particle, the determination of the mixing probability is more uncertain.[14]

The average Q value obtained for ^{35}S decay is 166.7 ± 0.2 keV, where the error reflects primarily uncertainties in evaluating electron energy corrections due to the dead layer on the detector. This value is in good agreement with the value given in the tabulation of atomic masses by Wapstra and Audi.[36]

B. Previous ^{35}S experiments

To the best of our knowledge, there have been five previous studies of the β spectrum of ^{35}S searching for a threshold anomaly 17 keV below the end point.[7–11] It is useful to have another look at these experiments because the present result and the tritium results both suggest that the intensity of the 17-keV neutrino branch that could explain this anomaly is only about 1%. Unfortunately all the reports of these experiments are quite brief, making detailed analysis difficult.

For comparison purposes with the other experiments, it is useful to note that in each of the runs in the present experiment there are about 6.5×10^5 counts/keV at the energy of the anomaly, 150 keV. As Fig. 7 shows, at the 10% level data of this statistical accuracy lead to a spread in $\sin^2\theta$ of ±0.004 and at the 1% level of ±0.006. Consequently, to rule out $\sin^2\theta$ of 0.006 at the 1% level requires statistical accuracy at least as good as obtained in one of the present runs.

Two types of experiments have been carried out previously, one using Si(Li) detectors much as in this work and the other using magnetic spectrometers of various types.

(1) Si(Li) experiments. Datar *et al.*[9] performed an experiment very similar to the present one. They claim to rule out a 17-keV neutrino with $\sin^2\theta<0.006$ at 90% confidence. However, judging from the error bars on their Fig. 1 there are only about 8×10^4 counts/keV at 150 keV in the spectrum. It is therefore clear that the experiment cannot rule out $\sin^2\theta$ of 0.006 at the 90% confidence level unless an important parameter has been held fixed or minimum χ^2 occurs at a nonphysical value of $\sin^2\theta$. One might guess that the accuracy would improve as the square root of the total number of counts and hence that this experiment cannot rule out $\sin^2\theta\leq0.011$.

Ohi *et al.*[8] have performed a similar type of experiment but incorporate a veto counter to reject some backscattered electrons. The use of a veto counter is a mixed blessing, because the backscattered electrons which should be vetoed and may not be are those that leave nearly their full energy in the principal detector. These backscattered electrons have low energy and cannot penetrate the dead layers on the entrance windows of the two detectors as well as the source substrate. This makes the tail on the electron response function very experiment dependent and difficult to compare with other, independent experiments. Ohi *et al.* quote a 90% confidence limit of 0.15% on $\sin^2\theta$. However, their spectrum has $\approx3.7\times10^5$ counts/keV at 150 keV, slightly more than one-half of one of the present runs. It is difficult to see how their 90% confidence limit could be better than about 0.5% unless they have constrained some parameters or unless the minimum in χ^2 is at a nonphysical value of $\sin^2\theta$. One parameter which is critical, the electron response function, is estimated by a long extrapolation from a measurement of the 570-keV IC line of ^{207}Bi. There is no discussion on how sensitive their results are to this response function. Finally Ref. 12 points out that there appears to be a threshold at 150 keV which, if analyzed in a narrow energy region, suggests a "kink" which would agree with a 17-keV neutrino with $\sin^2\theta$ at the 1% level.

(2) Magnetic-spectrometer experiments. Three of the ^{35}S experiments use magnetic spectrometers of various types. One of the problems with magnetic spectrometers is that, even after making all of the myriad corrections usually required, one seldom obtains a β-spectrum shape which agrees with theoretical expectations. To analyze the spectra obtained, it is usual to multiply the Fermi theory by a polynomial in the β energy on the principle that all systematic distortions are "smooth." Unfor-

tunately both the values of the coefficients in the polynomials and even the number of terms required is arbitrary and nonunique, primarily because of the strong dependence of these terms on Q, which is not known in advance with enough precision to fix it. An example of this will be given below.

In addition, the argument is usually advanced that such smooth distortions, describable by polynomials, will not mimic or cancel the effect of a heavy neutrino. This is certainly correct for the "kink region" as defined in Sec. II. However, as we shall now show, information from the regions above and below the kink region is essentially lost.

Consider the effect of a shape correction $[1+\alpha(Q-E)]$ to the Fermi theory for allowed decay, where $\alpha(Q-E)\ll 1$ over the energy interval to be analyzed. The slope of the Kurie plot is

$$\frac{dK}{dE}\propto 1+\alpha(Q-E)$$

which is now energy dependent. As an example, consider the slope at $Q-E=8.5$ keV relative to the slope at $Q-E=34$ keV. Then

$$\frac{(dK/dE)_{8.5}}{(dK/dE)_{34}}=\frac{1+8.5\alpha}{1+34\alpha}\approx 1-25.5\alpha\ .$$

This relative slope, in the case of 17-keV neutrino emission with $\sin^2\theta=0.008$ is 0.996 [Eq. (5)]. Hence an $\alpha\simeq 1.6\times 10^{-4}$ keV^{-1} will give a comparable relative slope.

The linear term required in several experiments is much larger than this limiting value of $\alpha\approx 1.6\times 10^{-4}$ keV^{-1}. A useful way to see the effect of larger values of α is to compare the slope of the Kurie plot at energies Δ above and below the "kink" which is

$$\frac{(dK/dE)_{+\Delta}}{(dK/dE)_{-\Delta}}\approx 1-2\alpha\Delta\ .$$

Equating this to the asymptotic slope ratio for a heavy neutrino, $\cos\theta$, leads to the requirement that

$$2\alpha\Delta<1-\cos\theta$$

in order that the phenomenological slope change not overwhelm the slope change due to the heavy neutrino. As a concrete example, suppose that $\alpha\simeq 5\times 10^{-4}$ keV^{-1}. Then $\Delta<4.0$ keV. Thus the data should only be analyzed within about ± 4 keV of the kink to be sure that unexplained curvatures of the spectrum are not much larger than that caused by a heavy neutrino. (This simplified analysis breaks down for α values much larger than this because for a value of $M_2\geq 17$ keV, the slope near the end point of the heavy neutrino is steeper; see Fig. 1. There are also resolution effects which have not been considered.) The effect of analyzing a β spectrum which includes a heavy neutrino by using the Fermi theory without the heavy neutrino multiplied by a linear function of the energy, $1+\alpha(Q-E)$ is shown in Fig. 12. Evidently the incorrect analysis with a very small linear term, $\alpha=1.3\times 10^{-4}$ keV^{-1} distorts the shape function drastically leaving evidence of the heavy neutrino only in a narrow energy region about the threshold.

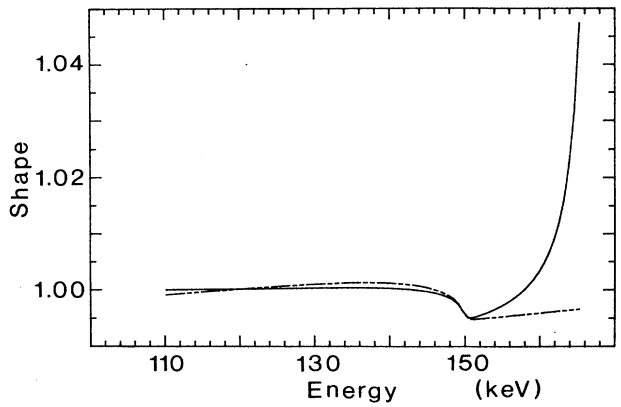

FIG. 12. Simulation of the effect of a linear term, $1+\alpha(Q-E)$ multiplying the Fermi theory. The smooth curve shows the ideal shape function for the case of $M_2=17$ keV and $\sin^2\theta=0.01$. The dashed curve shows the same data but now divided by the Fermi theory multiplied by $1+\alpha(Q-E)$ with $\alpha=1.3\times 10^{-4}$ keV^{-1}. Q has been varied to give a relatively smooth function.

In the experiment of Altzitzoglou *et al.*,[7] linear and quadratic terms bT and cT^2 relative to the constant term, where T is the electron kinetic energy, are required, with $b\simeq 2.6\times 10^{-3}$ keV^{-1} and $c\simeq -8.5\times 10^{-6}$ keV^{-2} for their particular choice of end-point energy. However this choice of end-point energy does not produce a shape function which has minimum χ^2 but only appears "smoothest" as can be seen by looking at their Fig. 3. Varying the end-point energy to obtain minimum χ^2 gives an extremely curved shape function, which cannot be well fitted with a quadratic polynomial but needs at least a cubic. This is an example of the nonuniqueness that can result from arbitrary shape factors. In any event, the coefficients of the polynomial are very large and certainly each term gives a slope change much larger than expected for $\sin^2\theta=0.008$. In view of the tremendous systematic distortion of their spectrum, their limit of $\sin^2\theta<0.4\%$ at 99% confidence seems overly optimistic.

In the experiment of Apalikov *et al.*[10] the data are fitted to the Fermi theory multiplied by $[1+\alpha(Q-E)][1+\alpha'(Q-E)^2)]$. The arbitrary parameters are very large: $\alpha=2.40\times 10^{-3}$ keV^{-1} and $\alpha'=1.33\times 10^{-5}$ keV^{-2}. According to the discussion above, the product $2\alpha\Delta<1-\cos\theta$ leads to an energy range Δ about the kink which is useful for testing the neutrino mass of <1 keV. In fact, the authors do show an expanded Kurie plot extending from 148 to 152 keV and as pointed out in Ref. 2 there appears to be a visible distortion at about 150 keV in this plot, which is also observable in the figure of deviation, their Fig. 2, and which is certainly consistent with $\sin^2\theta\sim 1-2\%$. The magnitude of the distortions implied by the large α and α' values precludes a reliable analysis of a large portion of the β spectrum. Their quoted upper limit of $\sin^2\theta=0.17\%$ at the 90% confidence level is extremely over optimistic especially in view of the evident local distortion in the Kurie plot.

Markey and Boehm[11] contributed a report giving an upper limit of $\sin^2\theta=0.3\%$ at 90% confidence. Unlike

other magnetic spectrometers, they report that they did not have an extraneous shape factor necessitating polynomial corrections. Examination of their paper suggests one serious experimental problem which is not addressed. At the spectrometer focus a cooled Si(Li) detector is used. The spectrum of the response to IC electrons of 126.9 keV shows a main peak with a tail. The tail, which they attribute to backscatter from the detector, represents about 60% of the total distribution. This is about a factor of 3–4 higher than expected for normally incident electrons[23] and raises serious doubt about the experiment. For example, if lower-momentum electrons are getting through the spectrometer, including them in the analysis is tantamount to making the energy resolution of the spectrometer enormously worse, which would certainly wipe out any kink there might be in the data.

C. ^{63}Ni experiment

A very detailed report on the measurement of the β spectrum of ^{63}Ni ($Q \approx 67$ keV, $\log ft = 6.6$) was very recently published[13] claiming an upper limit of 0.3% for $\sin^2\theta$ of a 17-keV neutrino consistent with the earlier claims from the ^{35}S experiments discussed above. This paper is worth reading to obtain a full grasp of the tremendous number of large corrections which must be made in many magnetic-spectrometer measurements. One large correction required is for imperfect transmission through the proportional counter's window which varies in a very nonlinear way by 10% over the region of the spectrum measured, 27–67 keV. The experiment also employs an "infinitely" thick source backing. In spite of the tremendous attention to detail described in this paper, a shape "correction" of the form $(1+\alpha E)$ was deemed to be required to fit the spectrum over the range 27–67 keV with $\alpha \approx 0.0006$ keV^{-1}. From the analysis previously given, such an α overwhelms the slope change due to $\sin^2\theta = 0.008$, and implies that the analysis should be confined to an energy region of ± 3.3 keV about the "kink." In fact they do perform an experiment covering a limited scan, from about 46 to 54 keV. (Even over such a narrow region, window transmission effects vary by nearly 1%, but we are ignoring this additional uncertainty.) Unfortunately, they include an arbitrary shape factor in this limited region, with an even larger $\alpha = 0.000\,75$ keV^{-1}, which is sufficient to remove evidence of a 0.008% branch from their data, as can be seen by comparing this shape factor with the data of their Fig. 10(a). Thus an upper limit of 0.44% on $\sin^2\theta$ (90% confidence limit) as quoted for this narrow-scan region is much too stringent.

VI. CONCLUSION

Two measurements of the β spectrum of ^{35}S have been made using very different sources and source-detector distances. The analysis of both measurements gives very similar results; both measurements show a threshold anomaly which is described best by assuming that the electron neutrino has two mass components, a very light one (<40 eV) and a heavy one with mass of 16.9 ± 0.4 keV. The mixing of the two components is given by $\sin^2\theta = 0.0073 \pm 0.0009 \pm 0.0006$. The single-component neutrino hypothesis is rejected at the $(100 - 5.1 \times 10^{-4})$% confidence level.

The present results are in disagreement with the claims of previous groups measuring β spectra of ^{35}S and ^{63}Ni. In the present experiment all important systematic effects are understood and accounted for. This is not generally the case in the other experiments, and it can be argued that, with the possible exception of two of the previous ^{35}S measurements,[8,10] these results are more correctly described as providing no support for a 17-keV neutrino at the 0.7% level rather than ruling it out. The two exceptions perhaps give weak confirmation of the 17-keV neutrino.[2,12]

The present result is remarkably similar to the results of the measurement of the β spectrum of tritium.[1,14] Since the β energy and the experimental technique are so different in the ^{3}H and ^{35}S measurements it would have to be a remarkable coincidence for extraneous experimental effects to produce the similar results. On the other hand, it has been shown that it is much more likely that improperly understood experimental effects can result in not recognizing a threshold in the data. Contrary to one's intuition, a null result is not more reliable than a positive result.

---

*Present address: Department of Nuclear Physics, University of Oxford, Nuclear Physics Laboratory, Keble Road, Oxford OX1 3RH, England.

[1] J. J. Simpson, Phys. Rev. Lett. **54**, 1891 (1985).

[2] J. J. Simpson, in *Massive Neutrinos in Particle Physics and Astrophysics,* proceedings of the Twenty-First Rencontre de Moriond (VIth Workshop), Tignes, France, 1986, edited by O. Fackler and J. Tran Thanh Van (Editions Frontières, Gif-sur-Yvette, 1986), p. 565.

[3] J. Lindhard and P. G. Hansen, Phys. Rev. Lett. **57**, 965 (1986).

[4] B. Eman and D. Tadić, Phys. Rev. C **33**, 2128 (1986).

[5] E. G. Drukarev and M. I. Strikman, Zh. Eksp. Teor. Fiz. **91**, 1160 (1986) [Sov. Phys. JETP **64**, 686 (1986)]; Phys. Lett. B **186**, 1 (1987).

[6] M. E. Rose, Phys. Rev. **49**, 727 (1936).

[7] T. Altzitzoglou, F. Calaprice, M. Dewey, M. Lowry, L. Piilonen, J. Brorson, S. Hagen, and F. Loeser, Phys. Rev. Lett. **55**, 799 (1985).

[8] T. Ohi, M. Nakajima, H. Tamura, T. Matsuzaki, T. Yamazaki, O. Hashimoto, and R. S. Hayano, Phys. Lett. **160B**, 322 (1985).

[9] V. M. Datar, C. V. K. Baba, S. K. Bhattacherjee, C. R. Bhuinya, and A. Roy, Nature (London) **318**, 547 (1985).

[10] A. Apalikov, S. D. Boris, A. I. Golutvin, L. P. Laptin, V. A. Lyubimov, N. F. Myasoedov, U. V. Nagovitsyn, E. G. Novikov, V. Z. Nozik, V. A. Soloshchenko, I. N. Tikhomirov, and E. F. Tret'yakov, Pis'ma Zh. Eksp. Teor. Fiz. **42**, 233 (1985) [JETP Lett. **42**, 289 (1985)].

[11] J. Markey and F. Boehm, Phys. Rev. C **32**, 2215 (1985).

[12] J. J. Simpson, Phys. Lett. B **174**, 113 (1986).

[13] D. W. Hetherington, R. L. Graham, M. A. Lone, J. S. Geiger, and G. E. Lee-Whiting, Phys. Rev. C **36**, 1504 (1987).

[14]A. Hime and J. J. Simpson, following paper, Phys. Rev. D **39**, 1841 (1989).
[15]B. Pontecorvo, Zh. Eksp. Teor. Fiz. **6**, 549 (1958) [Sov. Phys. JETP **33**, 429 (1958)]; **7**, 247 (1958) [**34**, 172 (1958)].
[16]Y. Katayama, K. Matsumoto, S. Tanaka, and E. Yamada, Prog. Theor. Phys. **28**, 675 (1962).
[17]Z. Maki, N. Nakagawa, and S. Sakata, Prog. Theor. Phys. **28**, 870 (1962).
[18]M. Nakagawa, H. Okonagi, S. Sakata, and A. Toyoda, Prog. Theor. Phys. **30**, 258 (1963).
[19]R. E. Shrock, Phys. Lett. **96B**, 159 (1980).
[20]B. H. J. McKellar, Phys. Lett. **97B**, 93 (1980).
[21]I. Yu. Kobzarev, B. V. Martemyanov, L. B. Okun, and M. G. Schepkin, Yad. Fiz. **32**, 1590 (1980) [Sov. J. Nucl. Phys. **32**, 823 (1980)].
[22]H. F. Schopper, *Weak Interactions and Nuclear Beta Decay* (North-Holland, Amsterdam, 1966).
[23]G. Knop and W. Paul, in *Alpha-, Beta- and Gamma-Ray Spectroscopy,* edited by K. Siegbahn (North-Holland, Amsterdam, 1965), p. 155.
[24]B. Planskoy, Nucl. Instrum. Methods **61**, 285 (1968).
[25]R.-D. von Dincklage and J. Gerl, Nucl. Instrum. Methods **A235**, 198 (1985).
[26]W. Bothe, Z. Naturforsch. **4a**, 542 (1949), quoted by Knop and Paul (Ref. 23).
[27]M. E. Riley, C. J. MacCallum, and F. Biggs, At. Data Nucl. Data Tables **15**, 443 (1975).
[28]H. A. Wyllie and G. C. Lowenthal, Int. J. Appl. Radiat. Isot. **35**, 257 (1984).
[29]ICRU Report No. 37, International Commission on Radiation Units and Measurements, Bethesda, Maryland, 1984.
[30]H. Behrens and J. Jänecke, *Landolt-Börnstein New Series* (Springer, Berlin, 1969), Group I, Vol. 4.
[31]*Table of Isotopes,* 7th ed., edited by C. M. Lederer and V. S. Shirley (Wiley, New York, 1978).
[32]L. Landau, J. Phys. USSR **8**, 201 (1944).
[33]S. Weisnagel and J. Law (private communication).
[34]M. S. Freedman, Annu. Rev. Nucl. Sci. **24**, 209 (1974).
[35]F. P. Calaprice and D. J. Milner, Phys. Rev. C **27**, 1175 (1983).
[36]A. H. Wapstra and G. Audi, Nucl. Phys. **A432**, 1 (1985).